MULTI-SPECTRAL DATA ACQUISITION AND PROCESSING TECHNIQUES FOR DAMAGE DETECTION ON BUILDING SURFACES

M. Hemmleb [a], F. Weritz [a], A. Schiemenz [b], A. Grote [c], C. Maierhofer [a]

[a] Federal Institute for Materials Research and Testing (BAM), 12200 Berlin, Germany (Christiane.Maierhofer@bam.de)
[b] AICON 3D Systems GmbH, 38114 Braunschweig, Germany (info@aicon.de)
[c] Institute of Photogrammetry and Geoinformation, 30167 Hannover, Germany (grote@ipi.uni-hannover.de)

Commission V, WG 2

Key Words: Cultural Heritage, Multispectral, Terrestrial, Laser Scanning, Classification, Acquisition, Detection, Recording

Abstract:

This paper describes the development and investigation of a multi-spectral laser scanner for non destructive diagnosis of damages on building surfaces. The application of four semiconductor lasers as defined active light source, especially in infrared wavelengths, allows the detection of damages like moisture, salt blooming and biological covering. Different methods for the evaluation of multi-spectral data for the analysis of damaged facades will be given. Whereas for preliminary statements vegetation and moisture indexes are applicable, further analysis is based on unsupervised and supervised pixel-based classification as well as object-oriented classification methods. An example clearly demonstrates the successful application of the multi-spectral laser scanner for the measurement of the relative moisture distribution on masonry. Additionally, different evaluations based on multi-spectral imagery from digital and infrared cameras (Vidicon) show the capabilities of multi-spectral techniques for the detection of damages on building surfaces.

1. INTRODUCTION

Precedent examination of building structures plays a crucial role for the planning of construction and restoration tasks. The multitude of possible damage of building surfaces makes manual damage mapping extensive and time-consuming. Therefore it is desirable to apply a method, based on image recording and processing for damage assessment, which also covers inaccessible parts of the building surface. It should also provide data for further analysis and classification of the existing damage. This approach offers good preconditions for automated damage detection. The surface structure and condition and especially its time-dependent changes have to be detected. Important damage of building surfaces are weathering, corrosion, salt blooming and biological changes like moss, lichen, moulds and moisture. The quantitative measurement of the moisture content has a particular importance, as most of the other damage is correlated with it.

Multi-spectral techniques offer the possibility to detect damage on building surfaces. Image regions can be assigned to affected (e.g. damaged by moisture or vegetation) surface regions. The dimension of the damaged area can be measured quantitatively. Therefore, the results of a multi-spectral analysis especially in the near infrared (NIR) can serve as a basis for damage mapping, delivering quantitative results on the damaged area and about the nature of the damage.

The main objective of the research project discussed in this paper was the development of a method providing images based on multi-spectral data acquisition with an active light source. The recorded data are processed with different software tools enabling multi-spectral classification. A multi-spectral laser scanner system was set up using four semiconductor laser diodes working at different wavelengths. From the difference in reflectivity, information about the surface condition and surface damage is gained. The use of semiconductor lasers as active light sources provides a better signal-to-noise ratio and allows reproducible measurement conditions. Thus quantitative measurement of the damage is possible.

2. MULTISPECTRAL TECHNIQUES FOR BUILDING DIAGNOSIS – AN OVERVIEW

Multi-spectral techniques depend on the measurement of the optical reflection of the investigated building surface with different wavelengths. If a broadband light source or surrounding light is used, separation of multi-spectral channels is normally based on optical filters. For that purpose, a camera is equipped with a filter wheel (Art Innovation, 2005) or with an electronic tunable filter (CRI, 2005; Mansfield, 2002). The used cameras should have no limits in respect to their spectral range. Then, with silicon-based CCDs a spectral range from about 400 nm to 1000 nm is available. In contrast, image acquisition in infrared range above 1000 nm needs special imaging devices. For this purpose, traditionally Vidicon cameras are used. They base on a sampling of an infrared-sensitive coating (for instance Lead Sulfide) with an electron beam. Nowadays, higher resolutions are reached with CCDs, based on infrared sensitive materials (Indium Gallium Arsenide), see for instance (Xenics, 2005).

As already mentioned, a more advanced approach is the application of a scanning system with active lasers as light source for reflection measurement. Experiences with 3D laser scanning help to establish a multi-spectral scanning device (Thomas, Wehr, 2005). The combination of a scanning measurement principle with reflection measurement in different wavelengths leads to a multi-spectral laser scanner. Unlike 3D laser scanners, at the moment multi-spectral laser scanners are not commercially available. Hence, for first measurements, a multi-spectral laser scanner was developed in the Federal Institute for Materials Research and Testing (BAM).

Independent of the result, every multi-spectral imaging device delivers two or more image channels – that means reflection data in a defined wavelength. Normally, evaluation of these

image channels is based on image processing algorithms known from remote sensing (for instance see Albertz, 2001). Multi-spectral classification is based upon distinct object classes, which show characteristic reflection behaviour as a function of wavelength. The transformation of the digitised intensities of n image channels (related to n wavelengths) of each point of the object into an n-dimensional feature space generates a cluster for each object class. If the classification is not supervised, these clusters are identified and marked off without any predefined knowledge. But using a supervised classification, predefined reference areas are considered and allow quantitative statements about the distribution of the object classes. Because of the high demands on classification methods for building surface diagnoses, especially object-oriented image classification methods promise good results. Some results are shown in chapter 4.

If preliminary statements are quickly needed, for instance for moisture and chlorophyll dissemination, they can be derived by the combination of selected image channels. For the calculation of the chlorophyll distribution the Normalized Difference Vegetation Index (NDVI) is used. It allows the identification and visualization of biological covering on the investigated building surface in an easy and effective way. According to the NDVI, the Normalized Difference Moisture Index (NDMI) can be processed (Equation 1). Here, the data recorded using the wavelength of the absorption line of free water (for instance at 1430 nm or 1940 nm) is related to data recorded at a reference line, which is insensitive to water. Thus, neglecting any further influences, the NDMI is a measure for the relative moisture content at the surface of the investigated structure.

$$NDMI = \frac{x_{Reference} - x_{Infrared}}{x_{Reference} + x_{Infrared}} \qquad (1)$$

Investigations of multi-spectral techniques for building diagnosis, especially in cultural heritage tasks, have been carried out for a long time. (Strackenbrock, 1990) and (Godding, 1992) used multi-spectral image classification for the analysis of different stone and damage types in architectural applications. By the combination of multi-spectral with multi-temporal images within a supervised classification, (Lerma, 2001) reaches enhanced results concerning the assignment of the detected classes with the real damage. Image Processing methods, like texture analysis and pattern recognition, give the possibility to apply extended information of the investigated object. (Lerma, 2000) and (Ruiz 2002) show, how this information as additionally image channels helps to increase the accuracy of the multi-spectral classification. New possibilities are given by the application of object-oriented classification methods, especially when considering the topology of the investigated object. (Neusch, 2003) shows the application of this approach on the evaluation of building facades.

As already mentioned, infrared optical methods give the possibility to detect moisture and also many other damage. Hence, infrared bands are very suitable for multi-spectral measurements of building damage. The effect of water absorption in different infrared bands was investigated in many cases, its utilisation for moisture measurement is pointed out by different authors (Böttcher, 1982; Geyer, 1995; Wiggenhauser, 2002). The combination of different infrared sensors, which enables a multi-spectral image evaluation is only sporadically applied, for instance for the inspection of sewers (Florin, 1999; Friedman, 2003) or the surface inspection of wood (Nestler, 2000).

3. MULTI-SPECTRAL LASER SCANNER

3.1 Principle

The principle of a multi-spectral laser scanner can be described as follows: The building surface is irradiated with laser light of defined wavelengths. The reflected radiation is measured with suitable detectors, like wavelength-sensitive photodiodes. Depending on the material, shape, condition and humidity of the surface, the reflected radiation has a varying spectral intensity distribution. In combination with a scanning system, the surface is covered grid-wise in predefined surface elements to capture the reflection characteristics. The measured data gained at the surface elements represent a multi-spectral image data set (image channels), which can be visualised and analysed with image processing techniques, especially with classification methods.

3.2 Set-up of the laser scanner

The developed laser scanner consists of four fibre-coupled semi-conductor laser diodes with different wavelengths, selected for the detection of moisture, natural cover and mineral changes. Considering the requirements for damage detection and the availability of laser diodes, the following wavelengths were chosen: 670, 808, 980 und 1930 nm (see Table 1). Suitable detectors based on Si and InGaAs photodiodes in combination with optical filters are used for the measurement of the reflected radiation.

Wavelength	Information
670 nm	Mineral composition, effects of weathering, corrosion, salt blooming, chlorophyll absorption
808 nm	Minimum of chlorophyll absorption, reference for vegetation index
980 nm	Minimum of water absorption, reference for moisture measurement
1930 nm	Water absorption band at 1940 nm

Table 1. Used wavelengths.

For the realisation of a scanning measurement system, two different devices were selected and tested under laboratory conditions: a pan-tilt-unit as carrier for the multi-spectral-head (as shown in Figure 1 and 2) and a mirror-scanning device, as known from 3D laser scanners. Geometric and radiometric calibration experiments were carried out.
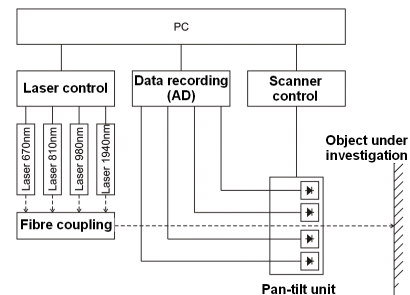

Figure 1. Set-up of the multi-spectral laser scanner with pan-tilt unit.

Measurement control and data recording is run on a notebook. The results are saved in a data file containing the intensity of the detected reflections for the different wavelengths for each pixel as well as the 2D geometric position. For data analysis, the reflection intensity of each channel, the NDVI and the NDMI are plotted automatically as a function of geometric position.

Additionally, the data can be saved in an output file, which can be directly used for enhanced multi-spectral classification with commercial software.
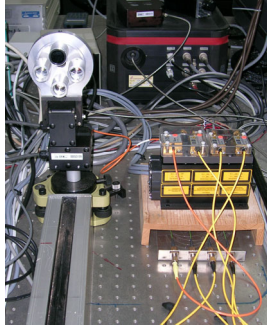

Figure 2. Left: Pan-tilt unit with measurement head, right: laser diodes and fibre coupling unit.

The first prototype of the multi-spectral laser scanner was set-up for laboratory investigation, and can principally be applied on-site, too. Further improvement is required for the robustness of the system, for the optimisation of the distance between measurement system and surface under investigation and for the measurement time per pixel, which can be drastically reduced by using the lasers in pulsed mode.

3.3 Geometrical calibration

Multi-spectral scanning, especially if used for multiple measurements requires a geometrical calibration of the used scanning system. Only a geometrical calibration enables the system to approach a defined point on the investigated surface. Besides, a geometrical calibration allows the transformation of the measured intensities from the used scanning coordinate system into an object coordinate system and therefore a correct mapping of the measured data.

In contrast to 3D laser scanners the developed multi-spectral laser scanner does not have the capability to measure object distances. Therefore the geometrical calibration and with it the geometrical model was developed for the scan of a planar object, like a building façade. The geometrical accuracy and stability of the pan-tilt-unit as well as of the mirror scanning device both in combination with the faser coupled red laser (670 nm) was investigated. For that purpose, the laser scanner was programmed to project a regular point pattern onto a perpendicular calibration plate. This projected pattern was acquired with a calibrated digital SLR camera (Olympus E20P) and evaluated by photogrammetric means. As a result, the object coordinates of the projected laser points were used for the laser scanner calibration. Camera calibration, photogrammetric image analysis and coordinate calculation within a bundle adjustment were performed with "Photomodeler" software by EOS Systems Inc.

The geometrical model for the pan-tilt-unit was found with:

$$
\begin{aligned}
x_i &= d \cdot \tan((p_i - p_0) \cdot \varepsilon_p) \\
y_i &= \frac{d \cdot \tan((t_i - t_0) \cdot \varepsilon_t)}{\cos((p_i - p_0) \cdot \varepsilon_p)} + \frac{a}{\cos((t_i - t_0) \cdot \varepsilon_t)} - a
\end{aligned}
\tag{2}
$$

where: x_i, y_i = object coordinates (in the calibration plane)
  p_i, t_i = position of scanner axis (pan, tilt)
  $p_0 = 0, t_0 = 0$, center position of scanner axis

  $\varepsilon_p, \varepsilon_t$ = angular resolution of the scanner
  d = object distance
  a = 89 mm, distance between tilt axis and optical axis

Using 49 laser points, the calibration, which is based on a least-squares-estimation, gives the following results:

$$\varepsilon_p = 0{,}05129°, \ \varepsilon_t = 0{,}05158°$$

The mirror scanning device demands a slightly varying geometrical model:

$$
\begin{aligned}
x_i &= d \cdot \tan((p_i - p_0) \cdot \varepsilon_p) \\
y_i &= \left(\frac{d}{\cos((p_i - p_0) \cdot \varepsilon_p)} + e \right) \cdot \tan((t_i - t_0) \cdot \varepsilon_t)
\end{aligned}
\tag{3}
$$

where: x_i, y_i = object coordinates (in the calibration plane)
  p_i, t_i = position of mirror axis
  p_0, t_0 = center position of mirror axis (32768, 32768)
  $\varepsilon_p, \varepsilon_t$ = angular resolution of mirror axis
  d = object distance
  e = 40 mm, distance between mirror axis

Again using 49 laser points, the calibration gives the following results:

$$\varepsilon_p = 0{,}0007426°, \ \varepsilon_t = 0{,}0007322°$$

With an object distance of 1,6 m the residues of the laser coordinates for both systems are at most 2 mm. One part of this residues is caused by remaining justage errors both of the scanners and the calibration plate. If using the above mentioned geometrical models, coordinate errors are under 1 mm for this object distance, which was sufficient for practical experiments with the multi-spectral laser scanner.

For the investigation of the stability of the scanning systems at least 16 scans with 25 laser points were carried out. After 8 scans all devices were switched off and on, meanwhile the position and other settings stayed constant. Positions of the laser beam were acquired in a period of 5 minutes. In contrast to the pan-tilt-unit, the mirror scanner needs a heating period of about 30 minutes. Table 2 gives an overview over the repetition accuracy of the investigated scanning devices with already heated systems. The maximal range is within the measurement accuracy using the above mentioned geometrical models and is sufficient for the application of multi-spectral measurements.

	pan-tilt-unit		mirror scanner	
	x (mm)	y (mm)	x (mm)	y (mm)
mean standard deviation	0,2	0,2	0,2	0,2
max. standard deviation	0,3	0,5	0,4	0,4
mean range	0,7	0,7	0,6	0,6
max. range	1,3	1,7	1,1	1,4

Table 2. Temporal geometrical stability of scanning systems for an object distance of 1,6 m.

3.4 Measurement results and discussion

After finishing the set-up of the multi-spectral laser scanner, test and calibration measurements were performed. First, the radiometrical and geometrical reproducibility and stability of the whole system was tested and approved. Together with these investigations, the limits and required parameters for application were determined. This was carried out through measurements of

the reflection properties of several different building materials (especially historic bricks and stones). As material parameters, the moisture content and the roughness of the surfaces have been varied (see Figure 3 and 4). For optimising the measurement parameters, the required power of the laser diodes and the distance of the scanner units to the measured surface were investigated systematically.
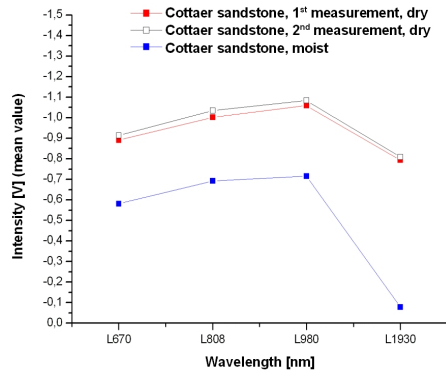

Figure 3. Intensity of reflection for dry and moist sand stone at different wavelengths. The wavelength axis is not scaled.
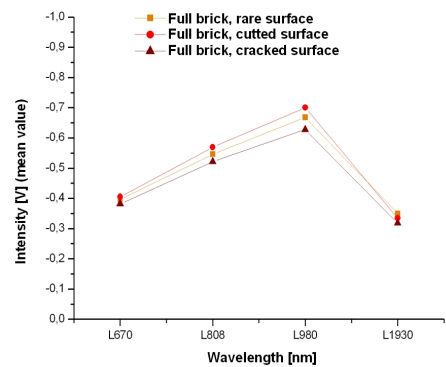
Figure 4. Intensity of reflection at different surfaces (roughness). The wavelength axis is not scaled.

A small test specimen (wall consisting of several small cut bricks in shape of cubes with a size of 5 x 5 x 5 cm^3) was investigated as shown in Figure 5. First, all bricks were measured in dry condition. Afterwards, two bricks were stored in water and the measurements were repeated for the determination of the moisture distribution at the surface. In addition to the four image channels for the four different wavelengths, also the NDMI was calculated from the reference wavelength (980 nm) and from the wavelength related to water absorption (1930 nm) as described above. The distribution of the NDMI is displayed in figure 6 as a false colour image. The area with enhanced moisture is clearly shown. At the bottom of the two moist bricks, water penetrated the joining dry bricks. Additionally, the differences in contrast due to varying surface properties recognized in Figure 5 outside the moist areas are not shown any more in Figure 6. The remaining small differences at the position of the edges of the bricks in Figure 6 and the increased NDMI at the bottom of the image are related to direct reflections of the laser radiation at the edges and to double reflections at the bearing surface of the test specimen, respectively. The NDMI given in Figure 6 is only a measure for the relative moisture distribution at the surface of the specimen. For the determination of the absolute moisture content, a calibration of the measurement system with a reference measurement method is required.

Figure 5. Wall consisting of small bricks, two of the bricks are moist. The photo was taken with a digital camera.
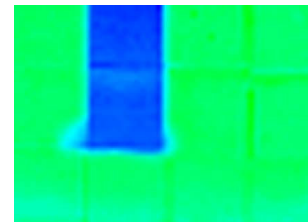

Figure 6. Distribution of the NDMI calculated from the multi-spectral scan and being a measure for the relative moisture distribution.

4 MULTI-SPECTRAL ANALYSIS BASED ON INFRARED AND DIGITAL CAMERA IMAGES

In addition to the multi-spectral measurements with the laser scanner, further objects were investigated with an infrared Vidicon camera including an adapter for suitable band-pass filters and with digital cameras. In principle, digital cameras are suitable for multi-spectral approaches, because they have three colour channels, which are needed at minimum for image classification. Furthermore CCDs are capable of acquiring radiation in near infrared with the red colour channel. These investigations were carried out to evaluate the commercial software packages for multi-spectral classification and to develop strategies for damage assessment at building surfaces.

4.1 Investigated objects

Damage on historical buildings frequently appears on facades with masonry or natural stones. Exemplarily a damaged masonry wall and a sand stone base wall were selected for the investigations. Figure 7 shows an evidently affected masonry wall. Damage like moisture and biological cover (moss) is clearly visible on the building surface. The region, selected for image acquisition, contains old and new bricks, dry and wet areas. As second investigation object a damaged sand stone wall was selected (Figure 9). Beside unaffected regions, damage like weathering, biological covering, salt blooming and contaminated areas is visible.

4.2 Image acquisition

Two different digital cameras were chosen for the image acquisition: First a simple Megapixel camera with a fixed focal length (Kodak DC3200) and second a professional 5 Megapixel SLR-camera with a zoom lens (Nikon D100). For image acquisition in infrared light, a Vidicon camera (Hamamatsu C2400-03) was equipped. The camera includes an adapter for suitable band-pass filters. Regarding the selection of appropriate filters it has to be considered, that they have a minimum bandwidth to get a feasible signal-to-noise ratio in the image data. Furthermore, attention has to be paid to the adjustment of the wavelength of the camera, the used lens and filters. Because of the

loss of power of the lens for higher wavelengths, in our case only six filters were used for the image acquisition and at last only four image channels with satisfying signal-to-noise ratio were selected (850, 900, 950, 1000 nm).

A commercial USB frame-grabber allowed the direct connection of the Vidicon camera with a notebook for straight-forward image acquisition. During image acquisition attention was paid to have diffuse illumination, ideally given by a cloudy sky. Using a lens with a focal length of 23 mm, the object distance was about three meters.

4.3 Multi-spectral data evaluation

At first, both multi-spectral image data of the digital camera (with three channels, RGB), as well as of the Vidicon camera (with four channels, see above) were evaluated separately with a multi-spectral image classification. Whereas the processing of digital camera image data already yields to feasible results, processing of Vidicon image data gives unsatisfying results. The reason for this is a small overall bandwidth and the correlation between the channels caused by the necessary broad bandwidth of the used filters. In order to get better results, digital camera data and infrared image data were used together in one classification. For this purpose, the infrared data set was transformed onto the other image data with a second order polynomial transformation together with bilinear image interpolation. Because of the high correlation between the infrared image channels, a principal component analysis (PCA) was performed.

In case of the masonry wall a channel with the vegetation index was calculated by use of the red and the 850 nm channel. Additionally a texture channel, containing the homogeneity criteria was calculated, in order to get more information about the object. Thus, for this investigation object up to six channels are available: RGB, infrared (PCA), NDVI and texture (homogeneity).

Looking closer to the data of the sand stone wall, some details are different. Because of the low dynamic of the infrared images, the first component of PCA was selected for the calculation of the NDVI. The investigated sand stone surface has only small variations, which yields to a low variance of the calculated values in the texture channel. Hence, the calculation of the homogeneity channel has been omitted.
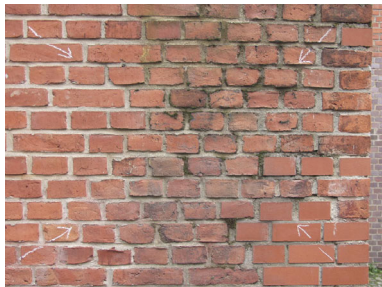

Figure 7. Damaged masonry wall, overview image taken with digital camera.

Figure 8a. Pixel-based unsupervised classification of masonry (cluster analysis).

Figure 8b. Pixel-based supervised classification (maximum-likelihood).
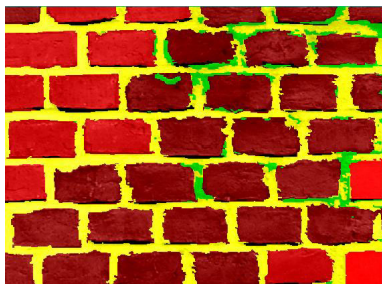

Figure 8c. Object-oriented classification, classification of the state of the bricks.

Figure 8d. Object-oriented classification, classification of damages.

Figure 9. Damaged sand stone wall, overview image taken with digital camera.
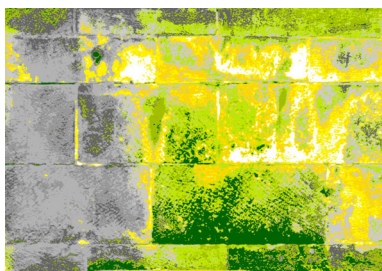

Figure 10a. Pixel-based unsupervised classification of sand stone (cluster analysis).
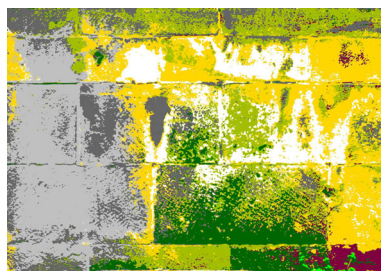

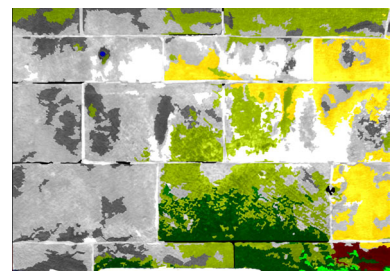Figure 10b. Pixel-based supervised classification (maximum-likelihood).

Figure 10c. Object-oriented classification of damages on sand stone wall.

Pixel-based classification methods as well as object-oriented approaches were utilized for multi-spectral data evaluation. Because of its robustness, a cluster analysis based on the ISODATA (iterative self-organizing data analysis technique) algorithm implemented in ERDAS Imagine, was chosen for pixel-based unsupervised classification. Also from ERDAS Imagine a module for supervised classification was selected, which is based on the maximum-likelihood-approach. As software for object-oriented multi-spectral classification we used eCognition.

4.4 Results and discussion

Masonry wall: Figure 8a/b shows the results of the pixel-based classification of the masonry wall. While unsupervised classification partly yields to incorrect results, especially in shadow regions, the supervised classification of biological covering (green) gives good results, because the chlorophyll absorption is measured very well by the infrared data. It has to be considered, that moisture content isn't covered by a water absorption line, that means, moisture is only covered by changes of spectral signature (light and dark blue). Object-oriented classification delivers similar results. In contrast to pixel-based classification, bricks, mortar and damaged areas are covered separately in discrete objects. The additional information from the texture channel allows the classification of the state of the bricks (old, new, damaged; see Figure 8c). Beside moisture and biological covering, salt blooming is detected and visualized in a separate class (see Figure 8d).

Sand stone wall: The results of the pixel-based classification of the sand stone wall are shown in Figure 10a/b. In contrast to the widely preserved sand stone (yellow), damage like biological covering (green), weathering (grey) and salt blooming (white) is clearly visible. In case of a supervised classification (Figure 10b), in addition contaminated areas (brown) and vegetation in the foreground (light green) are recognizable. Because of insufficient results of object segmentation with texture filters, a joint map was used for the object-oriented classification in order to get separated stone objects. Thus, a delimitation of different sand stone cuboids and the subdivision in filled and open joints is possible. Results (see Figure 10c) are comparable to the results of the pixel-based classification. In both cases, the classification between preserved and weathered sand stone is difficult.

5. CONCLUSIONS

The performed investigations clearly show that damage of building surfaces, caused by enhanced moisture content and/or vegetation, can be recorded automatically with a high signal-to-noise ratio by using the new developed multi-spectral laser scanner. The system allows further processing and analysis of the gained data and a damage evaluation and classification. This laser scanner prototype is the first available system using active illumination of the building surface for defined wavelengths. For enhancing the efficiency of the system, further developments are required to improve the robustness of the system and to reduce the needed time for data acquisition.

6. REFERENCES

Albertz, J., 2001. Einführung in die Fernerkundung. Wissenschaftliche Buchgesellschaft Darmstadt, 2. Auflage 2001.

Art Innovation, 2006. http://www.art-innovation.nl

Böttcher, B., Richter, H., 1982. Ein Beitrag zum Nachweis von Feuchtigkeit in Mauerwerk mit Hilfe einer Infrarotkamera. Materialprüfung Nr. 1, 24, pp. 5-9.

CRI, 2006. http://www.cri-inc.com/products/nuance.asp

Florin, C., 1999. Feuchtedetektion mit Hilfe der Infrarot-Technik. Feuchtetag 1999, DGZfP-Berichtsband BB 69-CD, P9, 1999, pp. 1-12.

Friedmann, M., 2003. Zerstörungsfreie flächenmäßig erfassbare Ortung von Hohlstellen und Feuchtigkeitsbelastungen mittels Infrarot-Thermografie. 14. Hanseatische Sanierungstage, Warnemünde, Schriftenreihe des Feuchte- und Altbausanierung e.V., Heft 14, 2003, pp. 61-70.

Geyer, E., Arndt, D., Günther, B., 1995. Bestimmung der Reflexion von trockenen und befeuchteten Baustoffen im Wellenlängenbereich 0,3 bis 2,5 µm für die IR-optische Bestimmung der Feuchte. Feuchtetag 1995, BAM, Berlin (1995) pp. 176-184.

Godding, R., Sacher, G., Siedler, G., 1992. Einsatz von digitalen Aufnahmesystemen zur Gewinnung von Multispektralaufnahmen für die Erkundung von Bauwerksschäden. In: International Archives of Photogrammetry and Remote Sensing, Com. V, New York, pp. 794-798.

Lerma, J. L., Ruiz, L. A., Buchon, F., 2000. Application of spectral and textural classifications to recognize materials and damages on historic building facades. In: International Archives of Photogrammetry and Remote Sensing, Vol. XXXIII, Part B5, Amsterdam, pp. 480-483.

Lerma, J. L., 2001. Multiband Versus Multispectral Supervised Classification of Architectural Images. Photogrammetric Record, Volume 17, Issue 97, pp. 89-101.

Mansfield, J. R., Attas, M., Majzels, C., Cloutis, E., Collins, C., Mantsch, H. H., 2002. Near infrared spectroscopic reflectance imaging: a new tool in art conservation. Vibrational Spectroscopy 28, 2002, pp. 59-66.

Nestler, R., Franke, K.-H., 2000. Realisierung eines multisensorischen Ansatzes zur Oberflächeninspektion von Holz. 6. Workshop Farbbildverarbeitung, GfaI, Berlin 2000.

Neusch, T., Grussenmeyer, P., 2003. Remote Sensing Object-Oriented Image Analysis Applied to Half-Timbered Houses. In: Proceedings of the XIX. International CIPA Symposium, Antalya, 4 pp.

Ruiz, L.A., Lerma, J. L., Gimeno, J., 2002. Application of Computer Vision Techniques to Support in the Restoration of Historical Buildings. In: International Archives of Photogrammetry and Remote Sensing, Com. III, Vol. XXXIV, Part 3A+B, 4 pp.

Strackenbrock, B., Sacher, G., Grunicke, J.-M., 1990. Image Processing for Mapping Damages to Buildings. In: Proceedings of the XIII. International CIPA symposium, Cracow, 7 pp.

Thomas, M., Wehr, A., 2005. Possibilities of multi-spectral laser scanners. Optical 3D-Measurement Techniques VII, Wien, 2005.

Wiggenhauser, H., 2002. Active IR-applications in civil engineering. Infrared Physics and Technology 43, pp. 233-238.

Xenics, 2006. http://www.xenics.com

7. ACKNOWLEDGEMENTS